ACS OMEGA

http://pubs.acs.org/journal/acsodf

Article

Effect of Fe−N Codoping on the Optical Properties of TiO_2 for Use in Photoelectrolysis of Water

Alvaro Realpe Jimenez,* Diana Nuñez, Nancy Rojas, Yulissa Ramirez, and María Acevedo

Cite This: *ACS Omega* 2021, 6, 4932−4938

Read Online

ACCESS | Metrics & More | Article Recommendations

ABSTRACT: TiO_2 nanoparticles were synthesized by green chemistry where organic solvents are replaced by an aqueous extract solution of lemongrass leaves that act as a reducer and growth-stopper agent. The nanoparticles were codoped with N−Fe to modify the absorption range in the electromagnetic spectrum and were characterized by Fourier-transform infrared (FTIR), scanning electron microscopy/energy dispersive X-ray spectroscopy (SEM/EDS), and UV−vis/diffuse reflectance spectroscopy (DRS). The modified samples with Fe and N resulted in smaller nanoparticle size values than pure TiO_2. Similarly, the band-gap energy for doped nanoparticles decreased to 2.22 eV in relation to the value of 3.09 eV for pure TiO_2, due to the introduction of new energy levels.

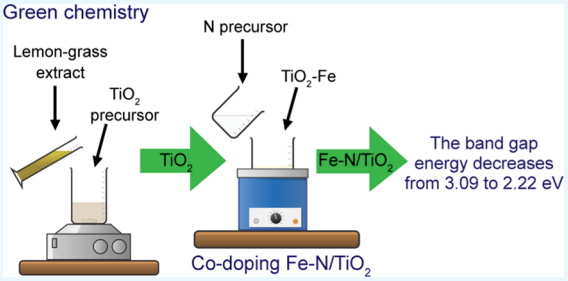

1. INTRODUCTION

Titanium dioxide (TiO_2) is characterized by being a photosensitive semiconductor, having good optical and electrochemical properties,[1] good dispersibility in organic solutions, and low toxicity.[2] These properties have led to numerous investigations directed to applications such as the removal of contaminants by photocatalysis[3−5] and photoelectrochemical devices for hydrogen generation.[6,7] TiO_2 can present several different phases in the nanometric range at different temperatures, which are anatase, brookite, and rutile, though anatase has excellent physical and chemical properties for environmental remediation.[8] However, the successful application of TiO_2 is still limited by its band gap energy[9] because the photoinduced reactions in TiO_2 are restricted to the UV region, which comprises only 4% of the solar spectrum.[10] Therefore, recent research aims to improve the optical and morphological properties of TiO_2, by codoping with different metal ion oxides in conjunction with nonmetals. This is due to the low rate of charge carrier recombination and the highly visible photocatalytic yield resulting from the synergistic effect of the codopant elements, compared to the results of doping with a single element.[11−14] Accordingly, in this work, TiO_2 codoped with Fe−N is prepared; the ionic radius of the N atom is close to the O atom in the TiO_2 lattice, resulting in the fusion of the N 2p orbital with the O 2p states, modifying the electronic structure of the valence band to easily transport load carriers.[15] Therefore, the simultaneous use of a metal and a nonmetal as codoping elements can be an effective modification. The aim of this research is to improve the optical and morphological properties of TiO_2 nanoparticles by codoping iron and nitrogen for hydrogen generation using a photoelectrochemical cell. Anatase phase TiO_2 nanoparticles were synthesized from a green synthesis mechanism by lemongrass extract; samples were prepared at different concentrations of Fe^{3+} and N, which have been characterized by scanning electron microscopy/energy dispersive X-ray spectroscopy (SEM/EDS), UV−vis, and Fourier-transform infrared (FTIR) spectroscopy.

2. RESULTS AND DISCUSSION

2.1. FTIR Spectra Analysis. FT-IR spectra analysis has been carried out to determine the functional groups present in the prepared samples (Figure 1). A strong absorption band is observed at the spectra of codoped TiO_2 (Figure 1b−d) between 3200 and 3400 cm^{-1}, corresponding to the stretching vibration mode of the hydroxyl bond (−OH), and the absorption band located around 1630 cm^{-1} can be assigned to the mode of bending of −OH vibration of absorbed water molecules in synthesized nanoparticles.[20] At low frequencies, a descent band in the range of 500−880 cm^{-1} has also been determined in all samples, corresponding to the Ti−O−Ti bond, indicating the formation of TiO_2.[2121] These patterns of vibrations are nearly similar to those identified in the unmodified TiO_2 sample, which are shown in Figure 1a. However, for codoped samples, in addition to the vibrations mentioned above, a peak in the wavenumber of 1082 cm^{-1} is

Received: December 8, 2020
Accepted: February 3, 2021
Published: February 11, 2021

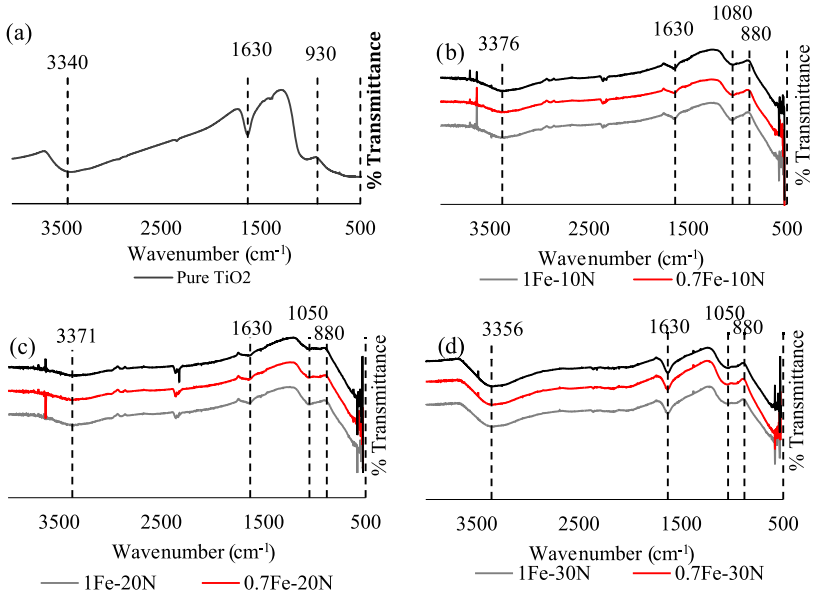

Figure 1. FT-IR spectra of (a) pure TiO_2 nanoparticles and Fe-doped TiO_2 nanoparticles at (b) 10%w/w N (c) 20%w/w N, and (d) 30%w/w N.

observed, which confirms the presence of a substituted N atom in the TiO_2 lattice, corresponding to the Ti−N vibration.[22,23] Also at low frequencies, a peak in 500−800 cm^{-1} can be attributed to the symmetric Fe−O−Fe stretching vibration.[24] The bond vibrations of the samples are in accordance with that reported in literature. In addition, for all codoped samples, characteristic peaks were observed at 500−880, 500−800, and 1082 cm^{-1}, confirming the presence of TiO_2, Fe, and N, respectively. The addition of Fe in the TiO_2 matrix results in changes that lead to the absorption of more amounts of OH groups.

2.2. SEM/EDS Analysis. The morphology of pure and Fe−N codoped TiO_2 nanoparticles has been determined through SEM images. Figure 2 shows the surface of the synthesized nanoparticles; a nonuniform distribution is observed. In addition, there are agglomerations in some regions, which can be attributed to the calcination treatment to which the nanoparticles were subjected.[25]

Furthermore, using ImageJ Software, it has been found that with Fe−N codoping, the size of the nanoparticles is in the range of 37−58 nm, as shown in Table 1, which is lower than the particle size of unmodified TiO_2 nanoparticles (70 nm),[18] whose SEM image is shown in Figure 2a. The decrease in particle size suggests that the codoping caused alterations in the structure of TiO_2, since the growth of the particle size is obstructed, which can be associated with the incorporation of Fe^{3+} ions in the crystal structure of TiO_2 due to differences in the atomic radius of Fe^{3+} and Ti^{4+}, as determined in the investigations of Othman and co-workers.[26,27] However, a significant trend of increasing concentration in nanoparticle size is not observed; the particle sizes reported by Realpe Jimenez et al.[18] were smaller when they were doped with Cu. The analysis shows that codoping radically affects the size of TiO_2 nanoparticles when is compared to the nondoped sample.

Peaks corresponding to O, Cl, Ti, and Fe have been found with the elemental chemical analysis EDS, as shown in Figure 3, indicating the formation of TiO_2.

Although the presence of Cl corresponds to ammonium chloride (the nitrogen precursor), no peaks have been detected for N, due to the detection limit of the EDS analysis for nitrogen, since there are interferences of lines of lighter elements superimposed with heavier elements.[28,29] The presence of Na, Mg, K, Ca, and V has also been identified; these lines are attributed to impurities or the equipment used.[25]

Table 2 shows the percentage by mass of iron, over the total sample, measured by EDS analysis, which indicates that Fe is incorporated into the TiO_2 support. A similar variation of the Fe concentration values given by EDS was observed by Kashale et al.[30]

2.3. UV−Vis Diffuse Reflectance Spectroscopy (UV−Vis/DRS). Figure 4 shows the optical properties of diffuse reflectance for pure TiO_2 and codoped with N and Fe TiO_2 in a wavelength range from 200 to 800 nm. For unmodified TiO_2, a wide absorbance band for wavelengths lower than 400 nm can be observed, which indicates that its range of photoactivity is limited to the UV region of the spectrum. However, for codoped samples, there is a shift of the absorption band toward wavelengths greater than 400 nm, and this shift increases with increasing Fe^{3+} concentration while N keeping constant (Figure 4k). Therefore, the valence band of the modified samples can be excited with photons of lower energy. On the contrary, absorbance decreases with increasing N concentration keeping Fe constant.

The band gaps of the modified samples were determined through the Tauc graphical method to analyze the optical properties of the nanoparticles, as shown in Figure 5 using eq 1.

$$(\alpha h\nu)^{1/n} = A(h\nu - E_g) \quad (1)$$

where α is the absorption coefficient, A is constant, $h\nu$ is the photon energy, E_g is the band gap, and n denotes the nature of the electronic transition interband. The variable n can have the values 1/2, 2, 3/2, and 3 corresponding to direct allowed, indirect allowed, direct forbidden, and indirect forbidden transitions, respectively. In this case, $n = 2$ for the indirect transition allowed to graph $(\alpha h\nu)^{1/2}$ vs $h\nu$.[31,32] Figure 5 shows the extrapolation of the linear part on the energy axis, obtaining the band gap of the synthesized samples.

https://dx.doi.org/10.1021/acsomega.0c05981
ACS Omega 2021, 6, 4932−4938

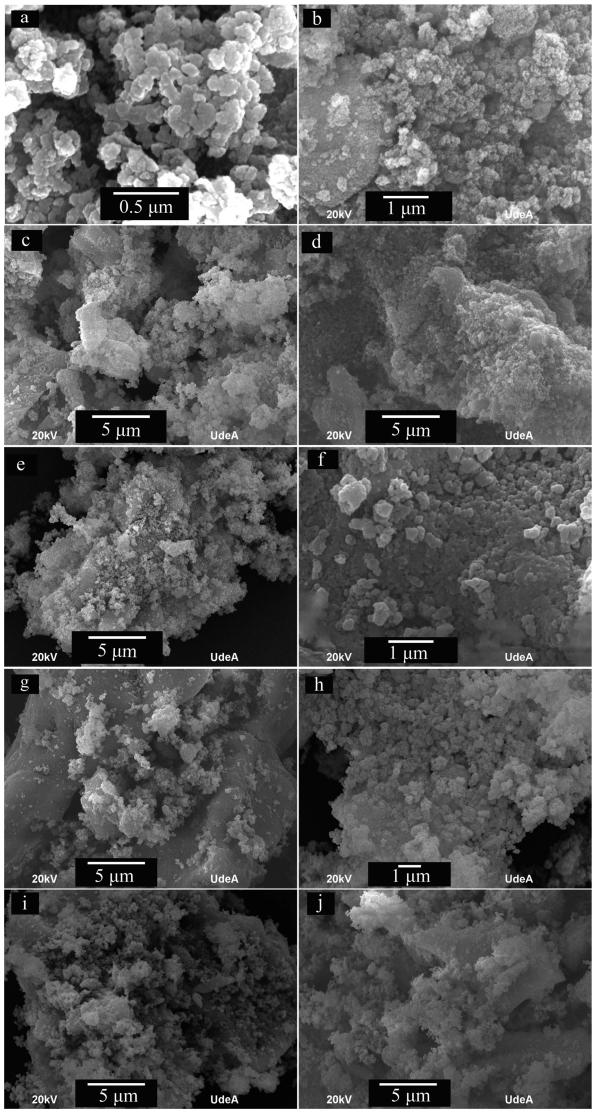

Figure 2. SEM images of pure TiO_2 and codoped TiO_2. (a) Pure TiO_2, (b) 1% Fe−10% N, (c) 0.7% Fe−10% N, (d) 0.5% Fe−10% N, (e) 1% Fe−20% N, (f) 0.7% Fe−20% N, (g) 0.5% Fe−20% N, (h) 1% Fe−30% N, (i) 0.7% Fe−30% N, and (j) 0.5% Fe−30% N.

Figure 6 shows the band gap for modified TiO_2 nanoparticles; these results were lower compared to the unmodified TiO_2 (3.09 eV). It is noted that when the percentage of Fe is kept constant, the band gap increases as the N concentration increased. On the other hand, when nitrogen percentage is kept constant, the band gap decreases as Fe percentage increased, which is consistent with the results found by Realpe Jimenez et al.[17] They worked with equal percentages (1, 0.7, and 0.5% w/w) of Fe, but performed only doping with Fe, concluding that the band gap decreases as the percentage of iron increases and obtaining their lowest band gap of 2.66 eV for 1.0% w/w Fe−TiO_2. However, in the current work, the lowest band gap of 2.22 eV was also found for TiO_2 codoping with 1.0% w/w Fe and 10% w/w N. This result supports the positive effect of doping with N. Furthermore, this entails that with doping there is a modification in the electronic structure of TiO_2, so that additional electronic states can be provided through Fe within the TiO_2 band gap.[33]

As reported by Ali et al.,[34] doping with Fe^{3+} in a TiO_2 lattice decreases the band gap due to the overlap of the conduction

Table 1. Particle Size of Synthesized Samples

	pure TiO_2 and codoped TiO_2									
	pure TiO_2	1% Fe−10% N	0.7% Fe−10% N	0.5% Fe−10% N	1% Fe−20% N	0.7% Fe−20% N	0.5% Fe−20% N	1% Fe−30% N	0.7% Fe−30% N	0.5% Fe−30% N
size (nm)	70	52	44	54	58	38	56	37	38	41

https://dx.doi.org/10.1021/acsomega.0c05981
ACS Omega 2021, 6, 4932−4938

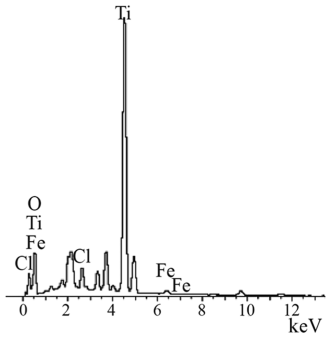

Figure 3. EDS spectra of TiO_2 nanoparticles codoped at 1% Fe−10% N.

Table 2. Percentage of Fe in Each Synthesized Sample Determined by EDS Analysis at Different Percentages of N and Compared to the Amount of Fe Initially Added

	amount of Fe measured by EDS at different N concentrations		
amount of Fe initially added	10% N	20% N	30% N
1% Fe	0.9% Fe	1.2% Fe	1.21% Fe
0.7% Fe	0.94% Fe	0.9% Fe	0.83% Fe
0.5% Fe	0.61% Fe	0.33% Fe	0.66% Fe

band due to the Ti (d-orbital) and metal (d-orbital) of the Fe^{3+} ions. Furthermore, the mechanism of the photocatalytic process in Fe-doped TiO_2 proposes that the Fe^{3+} ions induce the formation of new electronic states (Fe^{4+} and Fe^{2+}) that extend along with the TiO_2 band separation.

These electronic states can act as electron trapping sites and holes, and ultimately improve photocatalytic activity.[34] On the other hand, the influence of nitrogen in the decrease of the band gap is due to the fact that nitrogen can lead to a mixture of the N 2p orbital with the O 2p orbitals to form intermediate energy levels and move the absorption edge toward the visible light region.[35]

Finally, it should be noted that codoping with nitrogen and iron causes a stronger impact on the decrease of the band gap in comparison to the samples doped only with N or Fe^{3+} or not doped at all. As shown in the results found by Ali et al.,[34] the band gap of TiO_2 nanoparticles decreased when doped with Fe, but not down to the level achieved in this work. In other research, Nassoko et al.[35] performed N-doping, reaching a similar tendency of decreasing band-gap values per increment of N concentration. In addition, Grigorov et al.[36] found that doping N−TiO_2 decreases the optical gap; however, a similar behavior was presented, since, with the lowest concentration of N, the lowest band gap was reached. Likewise, this increment did not reach the level of the codoping with Fe and N, showing that codoping is favorable compared to just a single element because it maximizes the absorption range up to visible light. When comparing with other dopants, such as KI and Cu/S-codoped TiO_2,[37,38] it is observed that the band gap decreased more with Fe−N-doped TiO_2, extending the absorption to the visible light region even more than the other dopants.

3. CONCLUSIONS

TiO_2 nanoparticles codoped with Fe and N have been prepared at different concentrations by green chemistry using the lemongrass leave extract. The synthesized nanoparticles are explored for possible applications in photoelectrochemical cells. TiO_2 codoping shows a reduction in the particle size from 70 to 38 nm and the band gap energy from 3.09 to 2.22 eV with respect to the undoped TiO_2. Finally, the codoping method with Fe and N was successful, and FT-IR and EDS analyses reveal that these species are present in the samples. Therefore, the synthesis route of the codoped TiO_2 is interesting for its simple methodology and potential to synthesize various other nanocomposite materials.

4. MATERIALS AND EXPERIMENTAL SECTION

4.1. Materials. The materials used for the synthesis of titanium dioxide nanoparticles were titanium isopropoxide ($Ti[OCH(CH_3)_2]_4$, 95%, Alfa Aesar) as a titanium precursor and natural lemongrass extract as a reducing agent. Ethanol (C_2H_5OH, Chemi) was used to wash the nanoparticles. The codoping of the titanium dioxide nanoparticles was performed using ammonium chloride (NH_4Cl, Chemi) as a nitrogen precursor and nonahydrated ferric nitrate ($Fe(NO_3)_3{\cdot}9H_2O$).

4.2. Experimental Section. To obtain titanium dioxide nanoparticles, the process was divided into two stages, which began with the production of the natural lemongrass extract and subsequent reduction synthesis by means of a chemical reaction. For the preparation of the reducing extract, fresh leaves of lemongrass (*Cymbopogon citratus*) were washed with abundant distilled water, cut and dried in an oven at 60 °C; then they were cut into smaller pieces and milled. The infusion was prepared by immersion of 100 g of ground leaves in 500 mL of distilled water (0.2 g/mL) at a temperature of 90 °C. This extract was filtered several times to leave no solid residue and then concentrated by evaporation at 70 °C to 100 mL of solution.[16]

The titanium dioxide nanoparticles were made from a reduction mechanism, using a green chemistry process in which organic solvents are replaced by natural extracts. The nanoparticles were synthesized through the reduction of titanium tetra-isopropoxide (TTIP) with natural lemongrass extract. An aqueous solution of 850 mL of titanium tetra-isopropoxide at 10 mM was subjected to ultrasonic agitation for 30 min; then, 100 mL of lemongrass extract was added and subjected to magnetic agitation for 24 h at room temperature. The nanoparticles were separated by centrifugation at 3500 rpm for 15 min, and then, they were washed with ethanol and submitted to the same centrifugation conditions to be finally washed with distilled water and calcined up to 550 °C for 3 h, as reported by Realpe Jimenez and co-workers.[17,18] The nanoparticles of titanium dioxide were codoped using the wet impregnation method;[19] this process was divided into two parts, initially Fe^{3+} doping was performed and then doping with N. An aqueous suspension of the synthesized nanoparticles was subjected to ultrasound agitation for 30 min, and then an aqueous solution of nonahydrated ferric nitrate was added and ultrasound shaken for 1 h and then magnetic agitated with heating to 80 °C to evaporate the solvent (water). Finally, Fe-doped nanoparticles were calcined in a muffle at 400 °C during 2 h. For the N codoping of the TiO_2−Fe nanoparticles, the same method described above was used. The concentrations of both dopants were modified to determine their effect and interaction on the optical and charge-transfer capabilities of the photoelectrode. Thus, the factors studied are Fe doping, N doping, and the levels at which they are evaluated are the concentrations in % wt/wt with respect to the amount of TiO_2.

https://dx.doi.org/10.1021/acsomega.0c05981
ACS Omega 2021, 6, 4932−4938

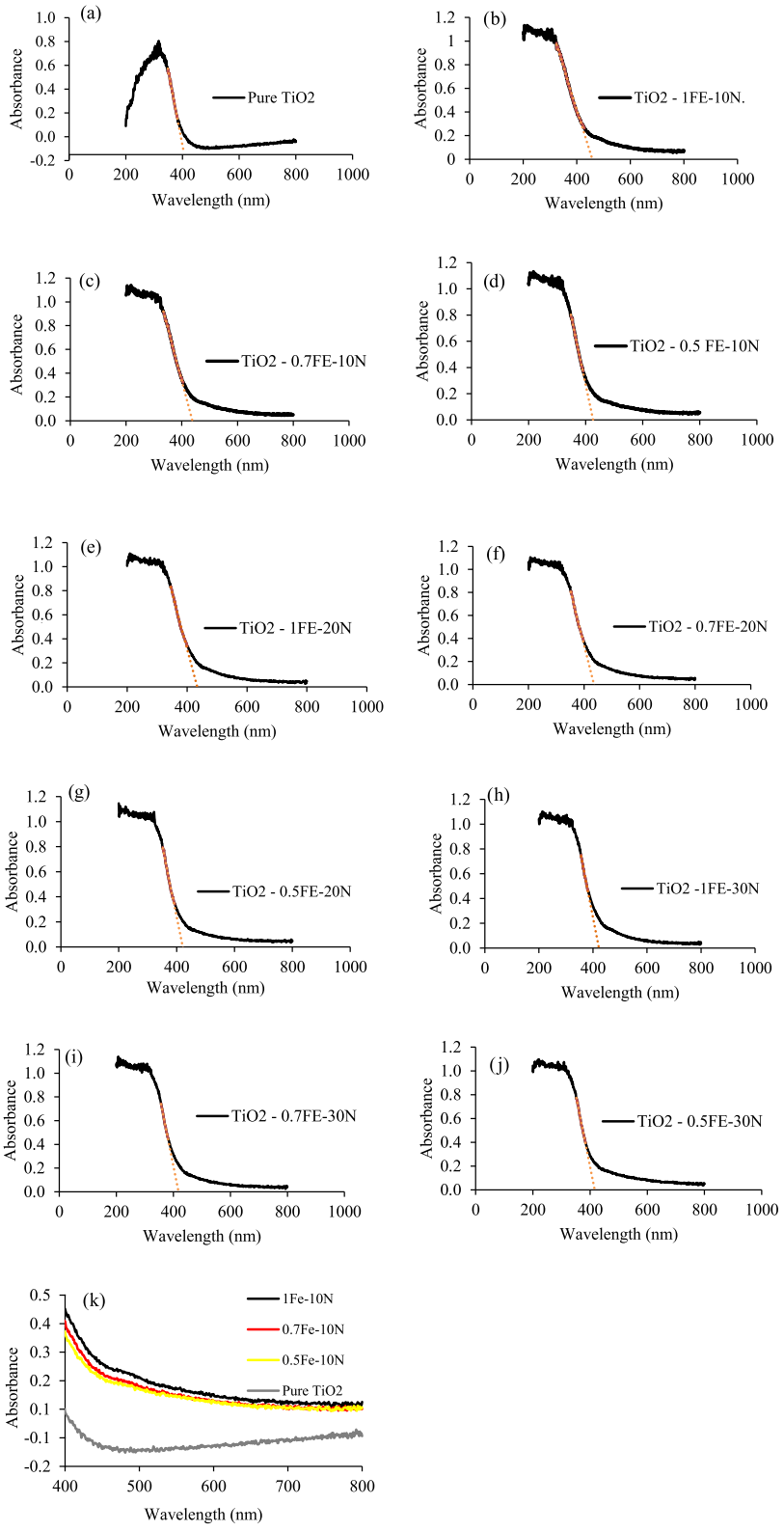

Figure 4. UV−vis diffuse reflectance spectroscopy (UV−vis/DRS) for the unmodified TiO_2 sample and TiO_2 modified with Fe^{3+} and N. (a) Pure TiO_2, (b) 1% Fe−10% N, (c) 0.7% Fe−10% N, (d) 0.5% Fe−10% N, (e) 1% Fe−20% N, (f) 0.7% Fe−20% N, (g) 0.5% Fe−20% N, (h) 1% Fe−30% N, (i) 0.7% Fe−30% N, (j) 0.5% Fe−30% N, and (k) N−Fe codoped TiO_2 at different Fe concentrations keeping 10% N to easily observe the change in absorbance.

4.3. Characterization. FT-IR spectra were performed to determine the functional groups present in the synthesized samples according to the characteristic peaks at different wavelengths between 500 and 4000 cm^{-1}. The size and morphology of the synthesized nanoparticles were determined through an SEM analysis using a JEOL JSM 540 scanning electron microscope. Finally, the spectrum of UV−visible diffuse reflectance was measured in the wavelength of 200−800

https://dx.doi.org/10.1021/acsomega.0c05981
ACS Omega 2021, 6, 4932−4938

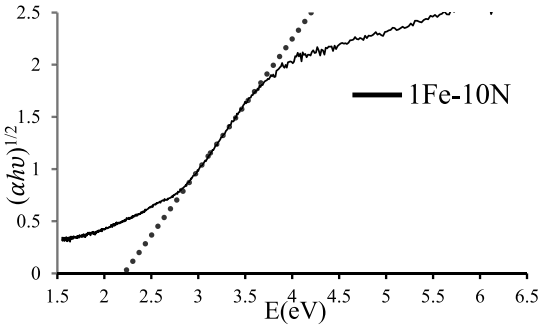

Figure 5. Band-gap TiO_2 samples modified with 1Fe−10N using the Tauc method.

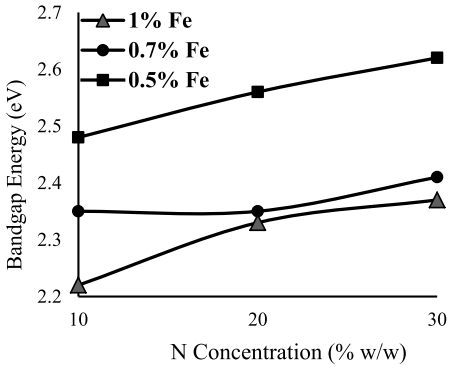

Figure 6. Band gap of the TiO_2 samples at different concentrations of Fe and N obtained by the Tauc method.

nm using a Thermo Scientific model EVOLUTION 600 UV/VIS spectrophotometer. This analysis allows determining the absorption range of the nanoparticles.

AUTHOR INFORMATION

Corresponding Author

Alvaro Realpe Jimenez − *Chemical Engineering Department, Particle and Process Modeling Research Group, Universidad de Cartagena, Cartagena 130015, Colombia;* orcid.org/0000-0002-0530-6573; Email: arealpe@unicartagena.edu.co

Authors

Diana Nuñez − *Chemical Engineering Department, Particle and Process Modeling Research Group, Universidad de Cartagena, Cartagena 130015, Colombia*

Nancy Rojas − *Chemical Engineering Department, Particle and Process Modeling Research Group, Universidad de Cartagena, Cartagena 130015, Colombia*

Yulissa Ramirez − *Chemical Engineering Department, Particle and Process Modeling Research Group, Universidad de Cartagena, Cartagena 130015, Colombia*

María Acevedo − *Chemical Engineering Department, Particle and Process Modeling Research Group, Universidad de Cartagena, Cartagena 130015, Colombia*

Complete contact information is available at: https://pubs.acs.org/10.1021/acsomega.0c05981

Notes

The authors declare no competing financial interest.

ACKNOWLEDGMENTS

This work was supported by the University of Cartagena (Resolution No. 031-2017).

REFERENCES

(1) Naresh Kumar Reddy, P.; Shaik, D. P.; Ganesh, V.; Nagamalleswari, D.; Thyagarajan, K.; Vishnu Prasanth, P. Structural, Optical and Electrochemical Properties of TiO_2 Nanoparticles Synthesized Using Medicinal Plant Leaf Extract. *Ceram. Int.* **2019**, *45*, 16251−16260.

(2) Inturi, S. N. R.; Suidan, M.; Smirniotis, P. G. Influence of Synthesis Method on Leaching of the Cr-TiO_2 Catalyst for Visible Light Liquid Phase Photocatalysis and Their Stability. *Appl. Catal., B* **2016**, *180*, 351−361.

(3) Hamadanian, M.; Reisi-Vanani, A.; Behpour, M.; Esmaeily, A. S. Synthesis and Characterization of Fe,S-Codoped TiO_2 Nanoparticles: Application in Degradation of Organic Water Pollutants. *Desalination* **2011**, *281*, 319−324.

(4) Islam, M. T.; Dominguez, A.; Turley, R. S.; Kim, H.; Sultana, K. A.; Shuvo, M. A. I.; Alvarado- Tenorio, B.; Montes, M. O.; Lin, Y.; Gardea-Torresdey, J.; Noveron, J. C. Development of Photocatalytic Paint Based on TiO_2 and Photopolymer Resin for the Degradation of Organic Pollutants in Water. *Sci. Total Environ.* **2020**, *704*, No. 135406.

(5) Zeng, X.; Sun, X.; Yu, Y.; Wang, H.; Wang, Y. Photocatalytic Degradation of Flumequine with B/N Codoped TiO_2 Catalyst: Kinetics, Main Active Species, Intermediates and Pathways. *Chem. Eng. J.* **2019**, *378*, No. 122226.

(6) Ansari, M. Z.; Singh, S.; Khare, N. Visible Light Active CZTS Sensitized CdS/TiO_2 Tandem Photoanode for Highly Efficient Photoelectrochemical Hydrogen Generation. *Sol. Energy* **2019**, *181*, 37−42.

(7) Yildiz, H. B.; Carbas, B. B.; Sonmezoglu, S.; Karaman, M.; Toppare, L. A Photoelectrochemical Device for Water Splitting Using Oligoaniline-Crosslinked $[Ru(Bpy)_2(BpyCONHArNH_2)]^{+2}$ Dye/IrO_2 Nanoparticle Array on TiO_2 Photonic Crystal Modified Electrode. *Int. J. Hydrogen Energy* **2016**, *41*, 14615−14629.

(8) Abisharani, J. M.; Devikala, S.; Dinesh Kumar, R.; Arthanareeswari, M.; Kamaraj, P. Green Synthesis of TiO_2 Nanoparticles Using Cucurbita Pepo Seeds Extract. *Mater. Today: Proc.* **2019**, *14*, 302−307.

(9) Munir, S.; Shah, S. M.; Hussain, H.; Ali Khan, R. Effect of Carrier Concentration on the Optical Band Gap of TiO_2 Nanoparticles. *Mater. Des.* **2016**, *92*, 64−72.

(10) Xiao, Q.; Si, Z.; Yu, Z.; Qiu, G. Sol-Gel Auto-Combustion Synthesis of Samarium-Doped TiO_2 Nanoparticles and Their Photocatalytic Activity under Visible Light Irradiation. *Mater. Sci. Eng., B* **2007**, *137*, 189−194.

(11) Apostolov, A. T.; Apostolova, I. N.; Wesselinowa, J. M. A Comparative Study of the Magnetization in Transition Metal Ion Doped CeO_2, TiO_2 and SnO_2 Nanoparticles. *Physica E* **2018**, *99*, 202−207.

(12) Khairy, M.; Zakaria, W. Effect of Metal-Doping of TiO_2 Nanoparticles on Their Photocatalytic Activities toward Removal of Organic Dyes. *Egypt. J. Pet.* **2014**, *23*, 419−426.

(13) Pouretedal, H. R. Visible Photocatalytic Activity of Co-Doped TiO_2/Zr,N Nanoparticles in Wastewater Treatment of Nitrotoluene Samples. *J. Alloys Compd.* **2018**, *735*, 2507−2511.

(14) Singaram, B.; Varadharajan, K.; Jeyaram, J.; Rajendran, R.; Jayavel, V. Preparation of Cerium and Sulfur Codoped TiO_2 Nanoparticles Based Photocatalytic Activity with Enhanced Visible Light. *J. Photochem. Photobiol., A* **2017**, *349*, 91−99.

(15) Thind, S. S.; Wu, G.; Chen, A. Synthesis of Mesoporous Nitrogen-Tungsten Co-Doped TiO_2 Photocatalysts with High Visible Light Activity. *Appl. Catal., B* **2012**, *111−112*, 38−45.

(16) Rajakumar, G.; Rahuman, A. A.; Priyamvada, B.; Khanna, V. G.; Kumar, D. K.; Sujin, P. J. Eclipta Prostrata Leaf Aqueous Extract

https://dx.doi.org/10.1021/acsomega.0c05981
ACS Omega 2021, 6, 4932−4938

Mediated Synthesis of Titanium Dioxide Nanoparticles. *Mater. Lett.* **2012**, *68*, 115−117.
(17) Realpe Jimenez, A.; Núñez, D.; Herrera, A. Synthesis of Fe-TiO_2 Nanoparticles for Photoelectrochemical Generation of Hydrogen. *Int. J. ChemTech Res.* **2016**, *9*, 453−464.
(18) Realpe Jimenez, A.; Nunez, D.; Acevedo, M. Effect of Cu on Optical Properties of TiO_2 Nanoparticles. *Contemp. Eng. Sci.* **2017**, *10*, 1539−1549.
(19) Nibret, A.; Yadav, O. P.; Diaz, I.; Taddesse, A. M. Cr-N Co-Doped ZnO Nanoparticles: Synthesis, Characterization and Photocatalytic Activity for Degradation of Thymol Blue. *Bull. Chem. Soc. Ethiop.* **2015**, *29*, 247−258.
(20) Mohamed, M. A.; Jaafar, J.; Ismail, A. F.; Othman, M. H. D.; Rahman, M. A. Fourier Transform Infrared (FTIR) Spectroscopy. In *Membrane Characterization*; Hilal, N.; Ahmad, I.; Takeshi, M.; Oatley-Radcliffe, D., Eds.; Elsevier B.V.: Ámsterdam, 2017; pp 3−29.
(21) Sharma, M.; Nihal. Effect of N-Doped Graphene on Optical, Electrical and Electrochemical Properties of Hydrothermally Synthesized TiO_2 Nanocomposite. *Mater. Today: Proc.* **2019**, *26*, 3390−3396.
(22) Sharotri, N.; Sharma, D.; Sud, D. Experimental and Theoretical Investigations of Mn-N-Co-Doped TiO_2 Photocatalyst for Visible Light Induced Degradation of Organic Pollutants. *J. Mater. Res. Technol.* **2019**, *8*, 3995−4009.
(23) Reda, S. M.; Khairy, M.; Mousa, M. A. Photocatalytic Activity of Nitrogen and Copper Doped TiO_2 Nanoparticles Prepared by Microwave-Assisted Sol-Gel Process. *Arab. J. Chem.* **2020**, *13*, 86−95.
(24) Tabasideh, S.; Maleki, A.; Shahmoradi, B.; Ghahremani, E.; McKay, G. Sonophotocatalytic Degradation of Diazinon in Aqueous Solution Using Iron-Doped TiO_2 Nanoparticles. *Sep. Purif. Technol.* **2017**, *189*, 186−192.
(25) Varma, R. S.; Baruwati, B.; Virkutyte, J. Doped Titanium Dioxide as a Visible and Sun Light Photo Catalyst. US Patent US8,791,044 B22014.
(26) Othman, S. H.; Abdul Rashid, S.; Mohd Ghazi, T. I.; Abdullah, N. Effect of Fe Doping on Phase Transition of TiO_2 Nanoparticles Synthesized by MOCVD. *J. Appl. Sci.* **2010**, *10*, 1044−1051.
(27) Othman, S. H.; Abdul Rashid, S.; Mohd Ghazi, T. I.; Abdullah, N. Fe-Doped TiO_2 Nanoparticles Produced via MOCVD: Synthesis, Characterization, and Photocatalytic Activity. *J. Nanomater.* **2011**, *2011*, No. 8.
(28) Hodoroaba, V.-D. Energy-Dispersive X-Ray Spectroscopy (EDS). In *Characterization of Nanoparticles*; Hodoroaba, V.-D.; Unge, W. E. S.; Shard, A. G., Eds.; Elsevier: Berlin, 2020; pp 397−417.
(29) Liang, D.; Liu, S.; Wang, Z.; Guo, Y.; Jiang, W.; Liu, C.; Wang, H.; Wang, N.; Ding, W.; He, M.; Wang, L.; Xu, S. Coprecipitation Synthesis of N, Fe Doped Anatase TiO_2 Nanoparticles and Photocatalytic Mechanism. *J. Mater. Sci.: Mater. Electron.* **2019**, *30*, 12619−12629.
(30) Kashale, A. A.; Dwivedi, P. K.; Sathe, B. R.; Shelke, M. V.; Chang, J. Y.; Ghule, A. V. Biomass-Mediated Synthesis of Cu-Doped TiO_2 Nanoparticles for Improved-Performance Lithium-Ion Batteries. *ACS Omega* **2018**, *3*, 13676−13684.
(31) Vijayalakshmi, R.; Rajendran, V. Synthesis and Characterization of Nano-TiO_2 via Different Methods. *Arch. Appl. Sci. Res.* **2012**, *4*, 1183−1190.
(32) Hossain, M. K.; Mortuza, A. A.; Sen, S. K.; Basher, M. K.; Ashraf, M. W.; Tayyaba, S.; Mia, M. N. H.; Uddin, M. J. A Comparative Study on the Influence of Pure Anatase and Degussa-P25 TiO_2 Nanomaterials on the Structural and Optical Properties of Dye Sensitized Solar Cell (DSSC) Photoanode. *Optik* **2018**, *171*, 507−516.
(33) Riaz, N.; Bustam, M. A.; Shariff, A. M. Iron Doped TiO_2 Photocatalysts for Environmental Applications: Fundamentals and Progress. *Adv. Mater. Res.* **2014**, *925*, 689−693.
(34) Ali, T.; Tripathi, P.; Azam, A.; Raza, W.; Ahmed, A. S.; Ahmed, A.; Muneer, M. Photocatalytic Performance of Fe-Doped TiO_2 Nanoparticles under Visible-Light Irradiation. *Mater. Res. Express* **2017**, *4*, No. 015022.
(35) Nassoko, D.; Li, Y. F.; Wang, H.; Li, J. L.; Li, Y. Z.; Yu, Y. Nitrogen-Doped TiO_2 Nanoparticles by Using EDTA as Nitrogen Source and Soft Template: Simple Preparation, Mesoporous Structure, and Photocatalytic Activity under Visible Light. *J. Alloys Compd.* **2012**, *540*, 228−235.
(36) Grigorov, K. G.; Oliveira, I. C.; MacIel, H. S.; Massi, M.; Oliveira, M. S.; Amorim, J.; Cunha, C. A. Optical and Morphological Properties of N-Doped TiO_2 Thin Films. *Surf. Sci.* **2011**, *605*, 775−782.
(37) Gupta, A.; Sahu, K.; Dhonde, M.; Murty, V. V. S. Novel Synergistic Combination of Cu/S Co-Doped TiO_2 Nanoparticles Incorporated as Photoanode in Dye Sensitized Solar Cell. *Sol. Energy* **2020**, *203*, 296−303.
(38) Shanthi, J.; Aishwarya, S.; Swathi, R. Enhanced Optical & Structural Properties by Potassium Iodide Doping on Spin Coated TiO_2 Thin Films. *Chem. Data Collection* **2020**, *29*, No. 100494.

https://dx.doi.org/10.1021/acsomega.0c05981
ACS Omega 2021, 6, 4932−4938